# Interhemispheric Anatomical Differences in Human Primary Auditory Cortex: Probabilistic Mapping and Volume Measurement from Magnetic Resonance Scans

V. B. Penhune[1], R. J. Zatorre[1], J. D. MacDonald[2] and A. C. Evans[2]

[1]Department of Neuropsychology and Cognitive Neuroscience and [2]McConnell Brain Imaging Centre, Montreal Neurological Institute and Hospital, McGill University, Montreal, Quebec, Canada

**The gyral morphology of the region of the primary auditory cortex (PAC) in the human brain is highly variable, and possible asymmetries between the hemispheres have been noted since the beginning of the century. We mapped the location and extent of PAC as identified from gross anatomical landmarks in magnetic resonance scans that had been transformed into Talairach–Tournoux stereotaxic space. Individual maps were averaged to produce a probabilistic map of the region which can be co-registered with any image of brain structure or function that has been similarly transformed. The map can be used to localize a region of interest, such as a lesion, or an activation focus from positron emission tomography or functional magnetic resonance imaging, within a specified range of probability. We also measured the total volume of the region and found a significant L > R asymmetry both on average and in the majority of subjects. Automatic segmentation of the volumes into grey and white matter revealed larger volumes of white, but not grey matter on the left. This larger volume of cortical connecting fibres may be related to the known left-hemisphere dominance for speech, and a preferential role for left PAC in processing temporal aspects of auditory stimuli is suggested.**

## Introduction

Highly specialized neural systems in the human brain allow the perception of complex auditory information such as that contained in music and speech. The cortical areas primarily responsible for auditory perception are located on the superior surface of the temporal lobe (Wernicke, 1874; Brodmann, 1909; vonEconomo and Horn, 1930; Celesia, 1976; Galaburda and Sanides, 1980). The gyral morphology of this region is highly variable and gross anatomical asymmetries between the hemispheres have been noted since the beginning of the century (Pfeifer, 1920; vonEconomo and Horn, 1930). Subsequently, numerous studies have examined interhemispheric differences in the planum temporale (PT), a region of secondary auditory cortex thought to be involved in speech perception (Geschwind and Levitsky, 1968; Witelson and Pallie, 1973; Steinmetz *et al.*, 1989b, 1990), but only a few have directly explored possible differences in primary auditory cortex (PAC) (vonEconomo and Horn, 1930; Rademacher *et al.*, 1993; Kulynych *et al.*, 1994). In the present investigation, we used magnetic resonance (MR) scans to map the location and to measure the volume of the region of the PAC from gross anatomical landmarks. The purpose of the study was twofold: firstly, to create a probabilistic map of PAC in a standardized stereotaxic space for the normal human brain; and secondly, to examine possible interhemispheric differences in the volume and location of the region.

The most common method for identifying regions of the brain, such as PAC, from an MR scan or functional image is the use of an atlas, such as that of Talairach and Tournoux (1988). This atlas is based on serial sections of a single brain, fitted to a standardized three-dimensional coordinate space based on midline landmarks. Talairach's development of a standardized space into which individual brain volumes can be translated has proved extremely important. At many centres, brain images obtained from MR and/or positron emission tomography (PET) are transformed into Talairach's standardized space in order to allow comparison with each other and with the atlas. Despite its widespread use, however, this approach has certain limitations. First, because it is drawn from a single subject, it cannot accommodate the range of individual variability in gyral morphology that exists in the population. In earlier work Talairach *et al.* (1967) themselves found considerable variability in the location of major sulci after transformation into the standardized space. While confirming the utility of a standardized space, Steinmetz *et al.* (1989a) found similar variability in a study using MR scans. Second, because only a single hemisphere is represented in each plane of section, possible interhemispheric differences in the location or extent of a given region cannot be assessed. Finally, because midline structures are used as the origins of the coordinate system, regions closer to the midline are better localized than more distant regions of the cortex. This means that the cortical regions which are often of greatest interest to clinicians and researchers are the least well localized.

In an effort to overcome these limitations, techniques have been developed to produce a probabilistic atlas of the human brain (Evans *et al.*, 1994). In the first step, a set of 305 magnetic resonance image (MRI) brain volumes were individually mapped into stereotaxic space, normalized for intensity and averaged to produce a finely sampled MRI composite (see Fig. 2, bottom panel; Evans *et al.*, 1992b). This data set illustrated anatomical variability in the human brain qualitatively, but did not yield quantitative measures. This paper is part of a second step, in which neuroanatomical variability is being examined quantitatively through a series of studies in which individual brain structures have been manually labelled (see also Collins *et al.*, 1995; Paus *et al.*, 1996). In this approach, the spatial uncertainty of the boundaries of a particular brain structure is expressed in terms of a probability map. In a probability map, each three-dimensional voxel in stereotaxic space is assigned a probability (0–100%) of being within the specified structure, based on its identification in a number of individual brains. A three-dimensional probability field is then built up from all the contributing voxels (see Fig. 2). The advantage of a probabilistic map is that it can be co-registered with any image of brain structure or function that has been transformed into stereotaxic space, allowing statistical assessment of the location of a region of interest. For example, it can be co-registered with the averaged image from a group of subjects, such as that produced via PET, functional MRI, magnetoencephalography (MEG) or electroencephalography, allowing a focus of activity to be localized within a specified range of probability. In individual

subjects, methods could be developed to localize a lesion, or to quantify the extent of a surgical removal.

While high-resolution MR scans of the whole brain allow clear visualization of cortical grey and white matter structures, they do not allow visualization of cytoarchitectonic features. Therefore, in order to identify the region of PAC from MR scans, it was first necessary to establish the existence of gross anatomical landmarks, visible on MR, which are reliably associated with the cytoarchitectonic boundaries. The auditory cortices are organized similarly to other sensory regions, with a central core of highly granular koniocortex surrounded by several less granular sensory cortical fields (vonEconomo and Horn, 1930; Galaburda and Sanides, 1980). The term PAC refers to the highly granular core region, whose cytoarchitecture is characterized by densely packed, small cell bodies with a distinct columnar organization and a high degree of myelination (Fleichsig, 1908; vonEconomo and Horn, 1930; Hopf, 1968; Galaburda and Sanides, 1980; Seldon, 1981a,b). This region has been variously identified as area 41 of Brodmann (1909), area TC of vonEconomo and Koskinas (1925) and the combined medial and lateral koniocortices of Galaburda and Sanides (1980). Since the turn of the century, neuroanatomists have agreed that PAC is located in the region of the transverse gyrus or gyri of Heschl (HG) on the superior surface of the temporal lobe (Brodmann, 1909; Pfeiffer, 1920; vonEconomo and Horn, 1930; Galaburda and Sanides, 1980). However, the gross morphology of this region is highly variable, both among individuals and between hemispheres. The HG region (HG-r) can contain from one to three gyri per hemisphere, and the number of gyri is not necessarily equal in both hemispheres (Pfeifer, 1920; vonEconomo and Horn, 1930; Campain and Minkler, 1976). Further, a single gyrus may be divided by a shallow sulcus which does not extend its full length, the sulcus intermedius (SI).

The degree of anatomical variability in HG-r made it initially unclear whether PAC could be reliably located relative to specific gross anatomical landmarks. Data from three previous studies are directly relevant to this question. vonEconomo and Horn (1930) mapped the auditory cortices from stained serial sections of 10 brains. Their drawings of individual subjects show PAC covering approximately the medial half of either the first, or the first and part of the second gyrus. Galaburda and Sanides (1980) collapsed data taken from three serially sectioned brains onto a schematic drawing showing a single left HG. This figure depicts PAC as confined to HG, and covering the central two-thirds of the gyrus. Most recently, Rademacher *et al.* (1993) mapped PAC from 10 serially sectioned brains with the specific intention of examining how well the cytoarchitectonic region fit gross anatomical boundaries. They found that when a single HG was present (14/20 hemispheres), PAC was always confined to that gyrus. When multiple gyri were present (6/20 hemispheres), PAC was almost always confined to the most anterior gyrus, and when HG was divided by an SI (7/20 hemispheres), PAC was confined to the anterior portion of the gyrus.

Functional localization studies in human subjects indicate that PAC is probably located on the medial portion of the most anterior HG. Recordings made from the surface of HG showed electrical evoked responses to clicks and pure tones over approximately the medial two-thirds (Celesia, 1976). Further, multisite depth-electrode recordings have shown that the early components of the auditory evoked response are generated from the medial portion of HG (Liégeois-Chauvel *et al.*, 1991, 1994). Evidence from PET imaging studies in normal subjects has shown specific activation of HG-r in response to basic auditory stimuli such as filtered white noise (Zatorre *et al.*, 1992) and has demonstrated its tonotopic organization (Lauter *et al.*, 1985).

The evidence from these studies, particularly the recent work of Rademacher *et al.* (1993), indicated that a reliable estimate of the location and extent of PAC could be made from gross anatomical landmarks. For the present study, this estimated region of PAC was defined as: the full extent of the most anterior HG, or the most anterior portion of that gyrus if it is divided by an intermediate sulcus (see Fig. 1 and Methods sections below). This region was designated PAC-r. Although functional mapping studies strongly suggest that PAC is located on the medial portion of the gyrus (Liégeois-Chauvel *et al.*, 1991, 1994), the lateral extent of PAC varies considerably (vonEconomo and Horn, 1930; Galaburda and Sanides, 1980; Rademacher *et al.*, 1993), and there is no gross anatomical guide to its end point. For this reason, it was decided that it was more reliable to mark the entire gyrus than to designate an arbitrary half-way point. Thus defined, PAC-r almost certainly includes auditory fields outside of PAC that are usually located on the lateral surface of HG [area 42 of Brodmann (1909); or PaAlt of Galaburda and Sanides (1980)].

The gross anatomical features defining PAC-r have been reliably identified from MR scans in a number of previous studies (Kulynych *et al.*, 1993, 1994; Steinmetz *et al.*, 1989b, 1990), in which the MR slice thicknesses used were comparable to those used in the present investigations. There are several additional features of the present investigations which should help to clarify the results of previous work. First, building on the work of Steinmetz *et al.* (1989b, 1990), we have used a consistent and reliable definition of the region of PAC, identifiable in MR scans. Second, differences in absolute brain size are controlled for by linear transformation of individual scans into stereotaxic space (Talairach and Tournoux, 1988; Evans *et al.*, 1992a; Collins *et al.*, 1994). Third, PAC-r is mapped by imaging the structure in the sagittal, horizontal and coronal planes of section simultaneously, using an interactive computer interface. Because this region is highly convoluted, and is bordered closely by regions of the parietal and frontal lobes, imaging in all three planes allows more accurate mapping than is possible with other MR techniques. Finally, the technique of probabilistic mapping in standardized space makes the information generated about the location and extent of PAC-r generalizable across individuals and groups. These data can be made available for use by other investigators, and the findings can be corroborated by studies in other laboratories.

The second goal of these experiments was to examine possible interhemispheric asymmetries in the region of PAC because previous investigations have yielded conflicting results (vonEconomo and Horn, 1930; Campain and Minkler, 1976; Galaburda and Sanides, 1980; Musiek and Reeves, 1990; Rademacher *et al.*, 1993; Kulynych *et al.*, 1994). In the present studies, no asymmetry was predicted *a priori*, but it seemed reasonable that mapping the region in a relatively large, normalized sample might reveal such differences if they were present. In these experiments, the total volume of PAC-r was measured by viewing the scans in three dimensions and labelling each voxel in the structure. Because the region is highly convoluted, the total volume measure includes portions of the structure not visible in other MR techniques, such as surface-rendering or slice reconstruction. In this respect, it is similar to measuring cortical extent from serial sections, with the important addition that white-matter volume is also included. In the second experiment, PAC-r volume measurements were repeated in a sample of higher-resolution MR scans and the total

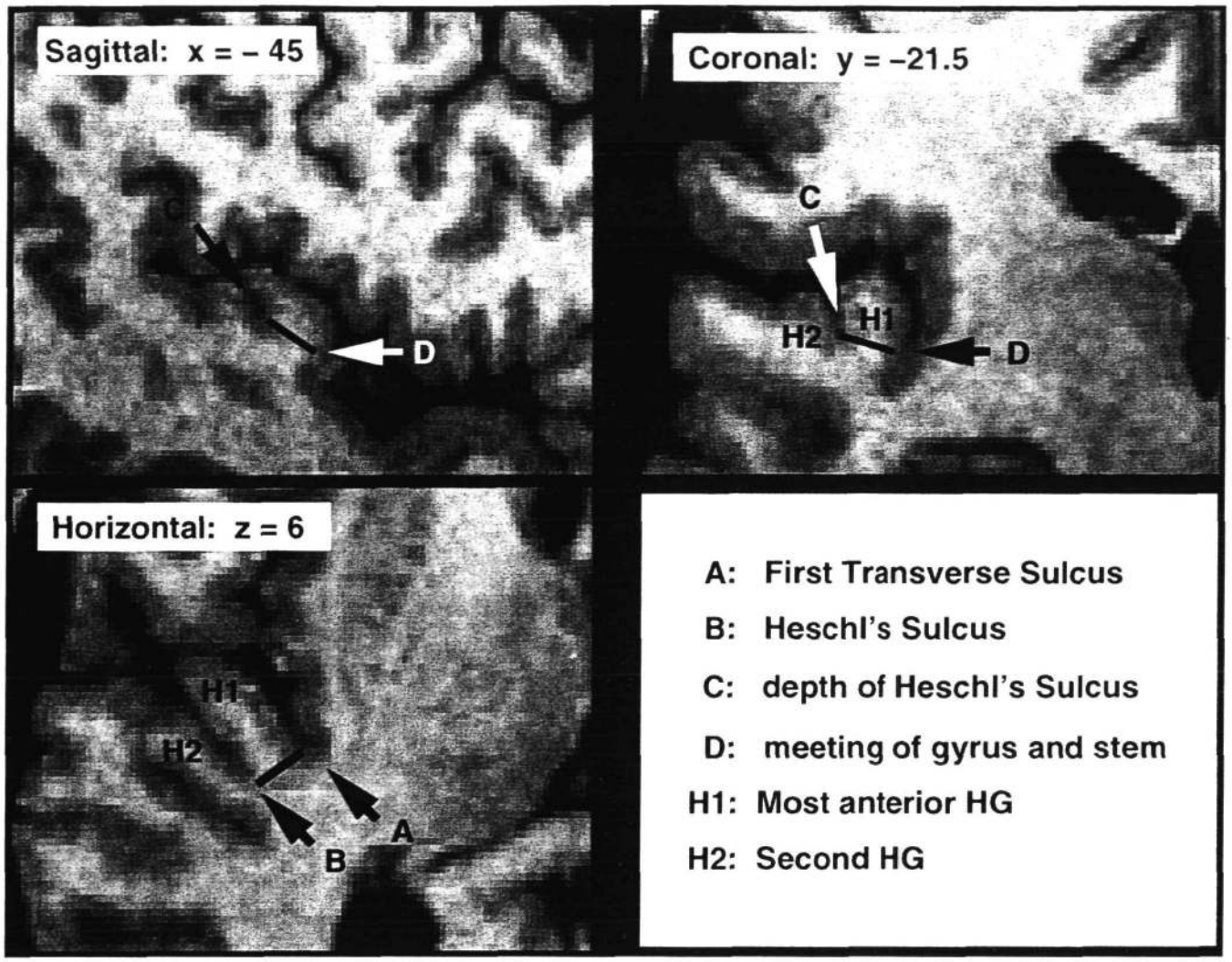


**Figure 1.** PAC-r landmarks and boundaries as visualized with DISPLAY in 1 mm scans. The posterior boundary (see horizonal section) is defined by HS (B), or by the SI when it extends at least half the length of HG. The posterior-medial boundary (horizontal section) is drawn between the medial end of the first transverse sulcus (A) to the medial end of Heschl's sulcus (B). The anterior-lateral boundary (horizontal section) is defined either by the visible ending of the gyrus (as in this case), or by extending the lines defined by A and B to the lateral border of the temporal plane. The inferior boundary (coronal and sagittal sections) is drawn from the depth of Heschl's sulcus (C) to the notch created by the meeting of the superior surface of HG and its stem (D). Slice levels were chosen to give the best view of the landmarks and are labelled in Talairach coordinates.

volume data were then automatically segmented by voxel intensity, allowing the grey and white matter volumes of PAC-r to be examined separately.

## Experiment I

### *Methods*

#### *Subjects*

The MR data used in the first experiment were drawn from a set of 305 scans of normal healthy volunteers (Evans *et al.*, 1992b) who underwent scanning as part of their participation in PET studies at the Montreal Neurological Institute (MNI). The sample included 12 males and 8 females, with a mean age of 23.5 (range 18–32). All were right-handed as assessed by self-report. Subjects were drawn from the McGill University and Montreal area population, were paid for their participation, and gave informed consent.

#### *MR Scanning and Data Manipulation*

Scans were performed on a Philips Gyroscan system with a 1.5 T superconducting magnet. Using a multiplanar spin-echo sequence, 64 contiguous 2 mm, $T_1$-weighted images were acquired in the axial plane ($T_R$ = 550 ms, $T_E$ = 30 ms). These data were then registered to the standardized stereotaxic space of Talairach and Tournoux (1988) using a linear resampling applied to a small set of anatomical landmarks manually identified in each scan (Evans *et al.*, 1992a). This standardized space defines three orthogonal dimensions related to the anterior and posterior commissures (AC and PC respectively) of the brain. These midline structures have a consistent relative location in the brain, and are clearly visible with a variety of radiological techniques (Talairach and Tournoux, 1988). A unique set of three coordinates in this system designates a unique location in the brain. The mediolateral, or $x$ dimension, extends from the midline to the lateral edge of the hemisphere, with negative numbers indicating the left hemisphere. The anterior-posterior, or $y$ dimension, extends from the plane drawn through the AC, with positive numbers anterior to the plane and negative numbers posterior. The inferior-superior, or $z$ dimension, extends from the horizontal plane

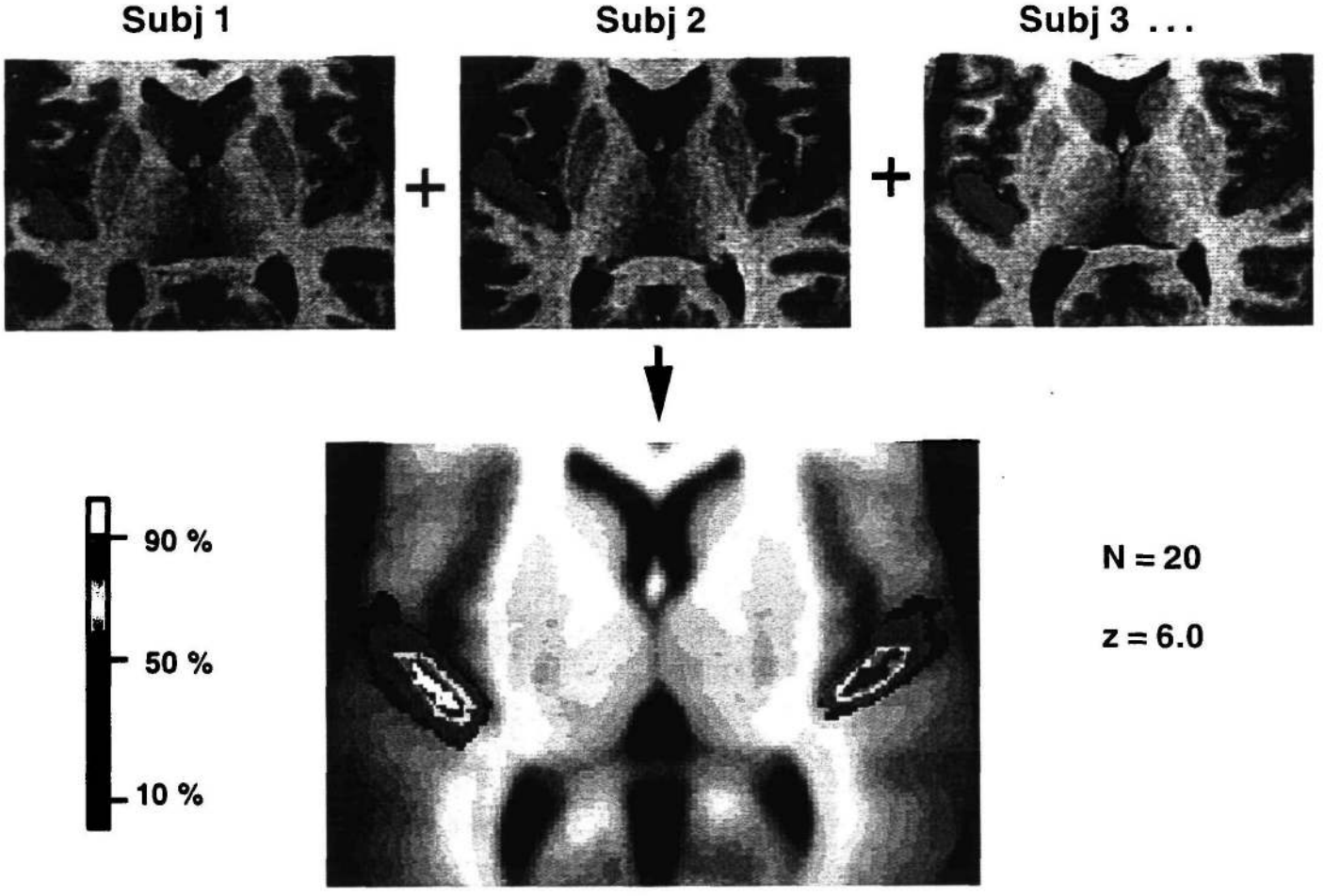


**Figure 2.** The top panel shows labelled volumes of PAC-r in the left and right hemispheres of three subjects (horizontal slices: $z = 6.0$). The labelled volumes are averaged across subjects, producing the three-dimensional probability map shown in the bottom panel. This map was generated from the high-resolution data ($n = 20$) and is co-registered with the average image of 305 MR scans in stereotaxic space ($z = 6.0$). The map scale represents the proportion of individuals for whom PAC-r was present at a given voxel location. Note that the area of the map is larger on the left, and that it is shifted anterio-medially on the right.

drawn through the AC and PC, with negative numbers inferior to the plane, and positive numbers superior. Resampling of MR volumes into stereotaxic space allows direct voxel-to-voxel comparison between the scans of two or more individuals. This resampling results in a volume of 160 axial slices with an in-plane matrix of 256 × 256.

*PAC-r Landmarks and Boundaries*

The gross anatomical landmarks and boundaries used to identify and mark PAC-r from the MR scans are shown in Figure 1. The anatomical terms and abbreviations used are: Heschl's sulcus (HS), the first transverse sulcus (TS) and the sulcus intermedius (SI). (i) The posterior boundary (see horizonal section): this boundary was defined by HS (B), or by the SI when it extended at least half the length of HG. (ii) The posterior-medial boundary (see horizontal section): a line was drawn from the medial end of the TS (A) to the medial end of HS (B). (iii) The anterior-lateral boundary (see horizontal section): this boundary was defined either by the visible ending of the gyrus (as in this case), or by extending the lines defined by TS and HS to the lateral border of the temporal plane. (iv) The inferior boundary (see coronal and sagittal sections): a line was drawn from the depth of HS (C) to the notch created by the meeting of the superior surface of HG and its stem (D). The inferior boundary is checked against the sagittal plane, where a second line was drawn from the depth of HS to D.

*Procedure*

The MR scans were viewed and marked using DISPLAY, an interactive three-dimensional imaging software package developed at the McConnell Brain Imaging Centre at the MNI (MacDonald *et al.*, 1994). This and other data analysis programs are run on SGI workstations. DISPLAY allows the scans to be viewed simultaneously in the coronal, horizontal and sagittal planes of section. When the mouse-controlled cursor is moved to any point in a given section, the program moves in real time to the corresponding view in the other sections. This feature is vital in identifying the borders of a three-dimensional object, such as HG, from two-dimensional slices. When the border of a region is viewed in a single section, it is not always clear whether all voxels belong to it or to a closely adjacent region. By allowing the observer to view the object in three planes simultaneously, a more accurate definition of the borders can be made.

In this experiment, PAC-r was identified and labelled by two raters (A.F. and V.P.). Overall intensity of the scans was set by visual inspection to give adequate grey/white contrast. The total volume of the region was labelled by marking all voxels within the boundaries described above in each continuous slice. PAC-r was labelled separately in each hemisphere, and the labels were stored as locations in stereotaxic space. The resulting label-volumes were used to create the three-dimensional probability map, to measure average location, and to calculate the total volumes. Figure 2 shows how the label-volumes are averaged across subjects to produce a three-dimensional map of the probability across the group that PAC-r will be found at a given location in stereotaxic space. The probability maps generated from the data in experiment I (2 mm slices) and the higher-resolution data in experiment II (1 mm slices) were qualitatively similar, and the average location of the region was also very similar (see

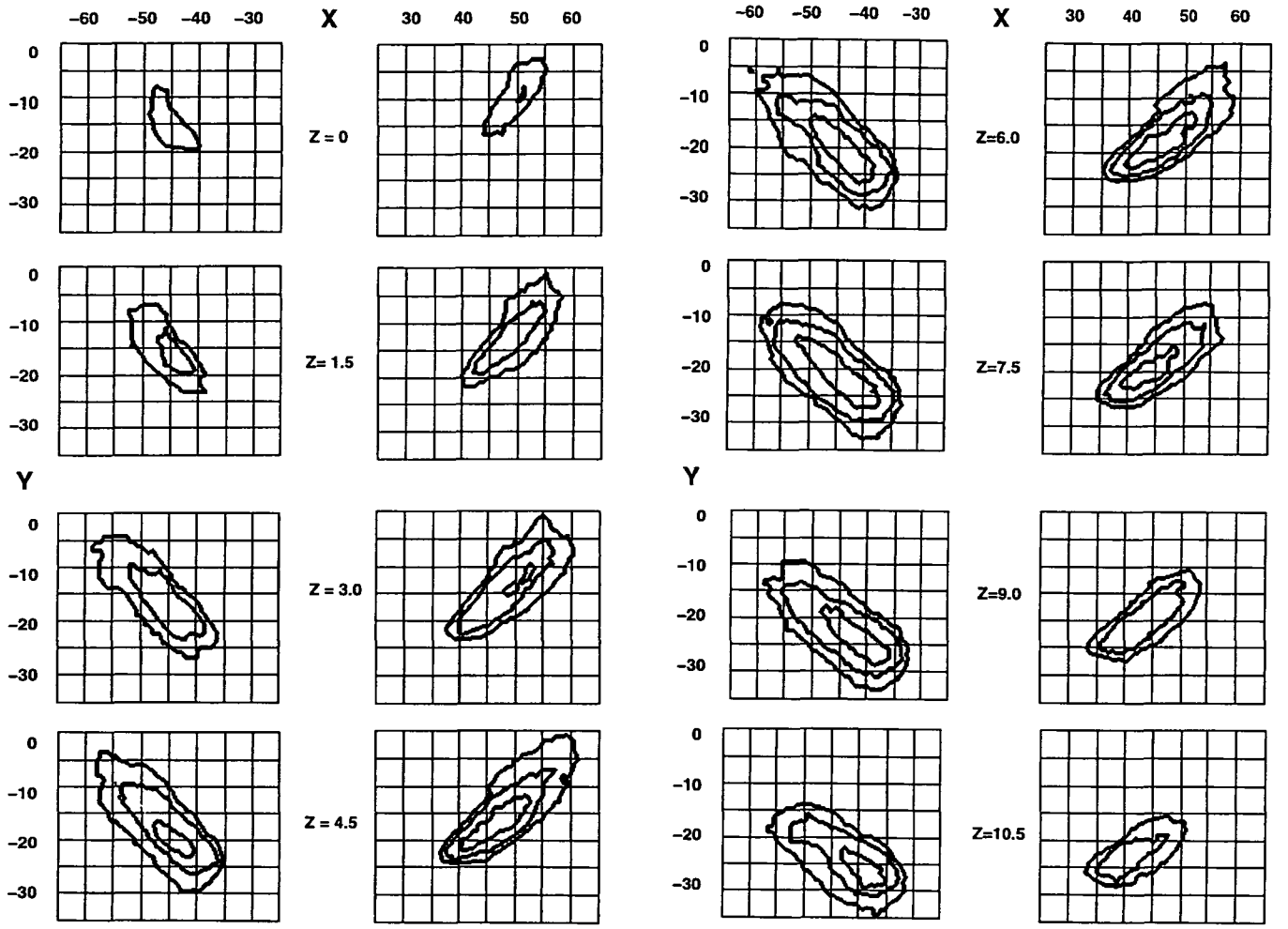


**Figure 3.** Probability contour maps at 25–50, 50–75 and 75–100% in 12 horizontal slices overlaid on a grid in standardized space ($z$ separation = 1.5 mm; range: $z$ = 0–16.5). In all slices, the outer contour represents 25–50%. When there are two contours, the interior contour represents 50–75%. When there are three contours, the interior contour represents 75–100%. Grid scale in mm; $x$ coordinates labelled horizontally, $y$ coordinates labelled vertically. The left hemisphere is represented on the left side of the page.

Table 1). Therefore, for precision, and to facilitate its use by other investigators, Figure 3 presents the probability map generated from the higher-resolution data in experiment II. Volume estimates for PAC-r were derived by multiplying the number of marked voxels in each hemisphere by the MR voxel dimensions ($x$ = 0.67 mm, $y$ = 0.86 mm, $z$ = 1.5 mm). Finally, the total number of gyri making up HG-r in each hemisphere were also noted.

## *Results*

### *Probabilistic Mapping*

As described above, averaging of the labelled volumes across subjects results in a three-dimensional map of the probability that PAC-r will be found at a given voxel location in stereotaxic space. Figure 3 presents contour maps for the regions of 25–50, 50–75 and 75–100% probability. Contour maps for 12 horizontal slices are overlaid on a grid in standardized space at 1.5 mm intervals. These contour maps can be used to localize a region of interest within PAC-r for a given range of probability. For instance, if a significant activation focus in a PET study was observed in the left hemisphere at $x$ = -50, $y$ = -20 and $z$ = 9.0, it would be found in the $z$ = 9.0 map within the 50–100% probability range.

One of the most important questions that can be asked about the probability map is how closely it matches the location of PAC-r as identified in the Talairach atlas. Preliminary examination of the map showed an apparent anterior-medial shift in the location of PAC-r in the right as compared to the left hemisphere. In order to investigate possible differences between the atlas and the map, as well as possible interhemispheric differences in the location of PAC-r, the bounding box (i.e. maximal extent in the $x$, $y$ and $z$ dimensions) for PAC-r was measured in each brain, averaged and compared with that determined from the Talairach atlas (Table 1). Average values were also compared between hemispheres using paired $t$-tests for dependent samples. The average location of PAC-r differs from the Talairach atlas in all three dimensions, particularly for the right hemisphere, which is not represented in the atlas, and whose location is assumed to be mirror-equivalent to that of the left. Differences in the $x$ and $y$ dimensions are most apparent for the right hemisphere, where the commencement of PAC-r is shifted ~8 mm anteriorly and ~6 mm medially from the values drawn from the atlas. The average location also differs bilaterally from the atlas in the $z$ dimension, where the most inferior point in PAC-r is 4–8 mm below that indicated in the Talairach atlas. Comparison between the hemispheres shows that the

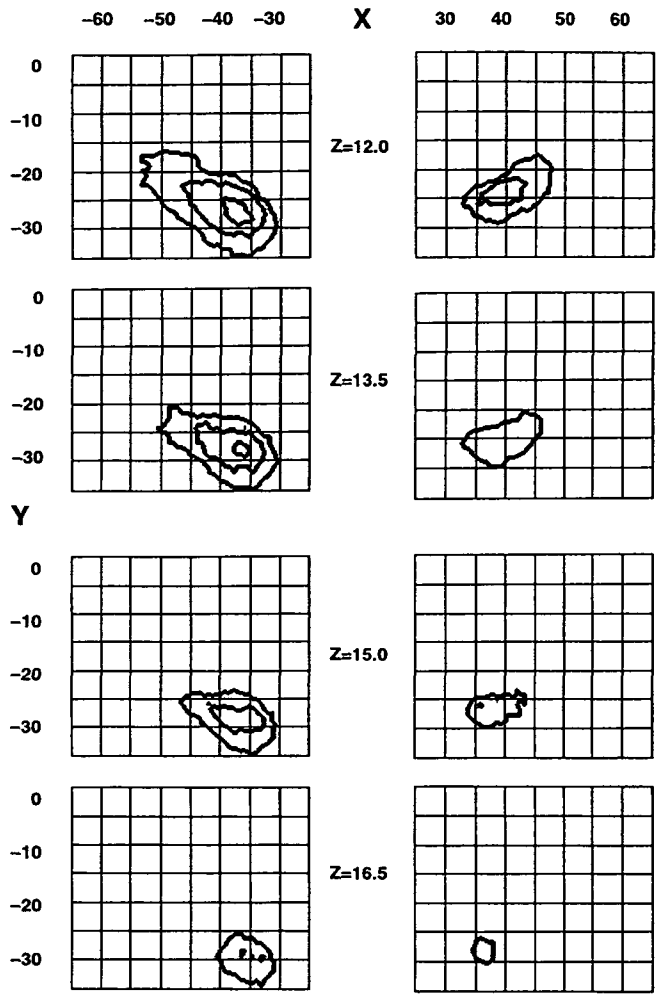


**Figure 3c**

commencement of right PAC-r is shifted an average of 6 mm anteriorly in the $y$ dimension ($L_{y,min}$ = -33.2, $R_{y,min}$ = -27.2, $t$ = -4.7, $P < 0.01$) and 2 mm medial in the $x$ dimension ($L_{x,min}$ = 32.9, $R_{x,min}$ = 34.7, $t$ = -3.6, $P < 0.01$).

*Interhemispheric Asymmetries*

In this experiment, the total volume of PAC-r was found to be larger in the left hemisphere both on average and in the majority of individual subjects. Analysis of variance (ANOVA) for repeated measures showed a significant effect of side [$F(1,18)$ = 21.8; $P < 0.0004$] that was unrelated to the sex of the subject [$F(1,18) = 0.94$; $P < 0.35$]. Inter-rater agreement for PAC-r volume was good as assessed by comparison of values for both raters in a subset of 10 scans (Pearson's linear correlation coefficient for left PAC-r, $r$ = 0.75, $P < 0.01$; right PAC-r, $r$ = 0.87, $P < 0.001$). Figure 4 compares the individual volumes of left and right PAC-r. A separate index of asymmetry, ∂PAC-r [$\partial\text{PAC-r} = (V_R - V_L)/(V_R + V_L/2)$] was calculated for each subject (cf. Rademacher *et al.*, 1993). Leftward asymmetries result in negative values, rightward asymmetries result in positive values; PAC-r was considered to be asymmetric when $|\partial\text{PAC-r}| > 0.10$. Individual PAC-r volumes and the index of asymmetry for each subject are reported in Table 2. The majority of subjects in this study had a left-sided asymmetry (17/20 subjects), while only a few had a right-sided or no asymmetry (R > L in 2/20 subjects; R = L in 1/20 subjects). The correlation of left and right PAC-r volumes approached significance ($r$ = 0.43, $P$ = 0.06).

Table 3 lists the possible gyral configurations of HG-r (i.e. the number of gyri per hemisphere), and gives frequency data for this and other studies in the literature. In the present sample the majority of subjects had only one gyrus in both hemispheres (14/20 or 70%). In the past, it has been stated that the most common morphological configuration of HG-r is one gyrus in the left hemisphere and two in the right (Pfeifer, 1920; Campain and Minkler, 1976). However, examination of these data indicates that the true frequency of this and other configurations appears to be quite variable.

### *Discussion*

Examination of the probability map and analysis of the bounding box data from experiment I reveal that PAC-r is located more anterio-medially in the right hemisphere. These differences, both between the hemispheres and from the Talairach atlas, confirm the importance of population-based mapping of the cerebral cortex.

The most striking result of this study was the consistent L > R asymmetry in the volume of PAC-r, a finding that was not predicted from the results of previous investigations. A L > R asymmetry in the gross extent of HG had previously been described (vonEconomo and Horn, 1930; Musiek and Reeves, 1990), and the recent work of Rademacher *et al.* (1993) showed a relative L > R asymmetry in cytoarchitectonic area of PAC. However, other studies have failed to show such an asymmetry, either in the surface area of the most anterior HG (Kulynych *et al.*, 1994) or in the area of PAC (Galaburda and Sanides, 1980); and a final study reported a R > L asymmetry for HG-r (Campain and Minkler, 1976). Our result was also not consistent with more traditional theories of neocortical organization (Flechsig, 1920; Luria, 1973), which have suggested that functionally significant anatomical asymmetries would occur only in secondary or association cortices, as has been observed in the PT.

Because the full volume of the region was measured in this study, the observed asymmetry could have resulted from greater volumes of cortical grey matter, white matter or both. Previous investigations of interhemispheric asymmetries in secondary auditory areas such as the PT have focused on differences in the extent or organization of cortical grey matter (Geschwind and Levitsky, 1968; Braak, 1978; Steinmetz, 1990), but have not examined possible differences in the underlying white matter. In order to examine the relative contributions of both tissue types to the observed asymmetry, and to replicate the results of experiment I, the same measurements were made in a second sample of subjects. These scans were acquired with a higher-resolution protocol, which made it possible to segment the total PAC-r volumes into grey and white matter components. Although sex did not affect the results of the first experiment, an equal number of male and female subjects were included in the second experiment in order to examine this issue more precisely.

## Experiment II

### *Methods*

#### *Subjects*

The MR data in the second experiment were drawn from a pool of normal, right-handed volunteers who had undergone scanning with the new three-dimensional acquisition protocol as part of their participation in PET studies at the MNI. This sample included 10 males and 10 females,

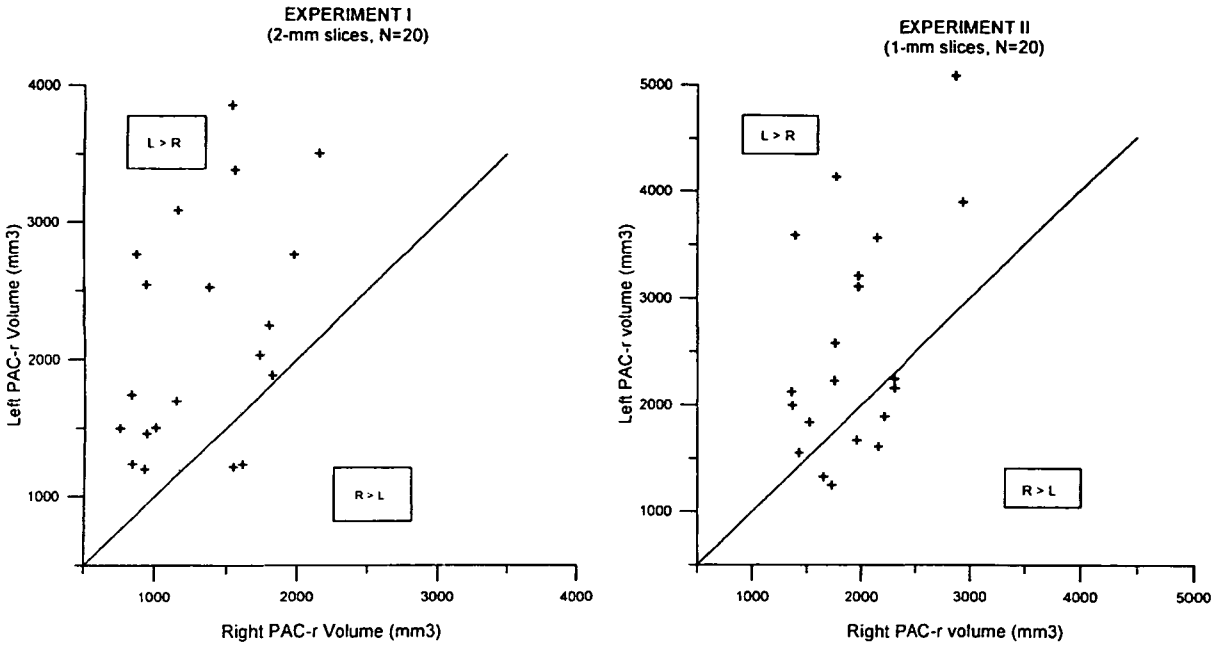


**Figure 4.** Scatterplots for left and right PAC-r volumes in experiments I and II. The solid line represents those values at which left and right volumes are equal. Points which fall above the line represent subjects for whom left PAC-r is larger than right; those which fall below the line represent subjects for whom right PAC-r is greater than left.

**Table 1**
Average minimum and maximum *x*, *y* and *z* values of PAC-r in stereotaxic coordinates for the two hemispheres and the Talairach atlas

| | | *x* dimension | | *y* dimension | | *z* dimension | |
|---|---|---|---|---|---|---|---|
| | | Min | Max | Min | Max | Min | Max |
| Experiment I | L | −32.9 ± 1.5[a] | −62.3 ± 4.3[a] | −33.2 ± 3.7[a] | −4.9 ± 6.1 | 1.4 ± 3.7 | 14.2 ± 4.1 |
| | R | 34.7 ± 2.1[a] | 58.2 ± 4.2[a] | −27.2 ± 3.9[a] | −2.1 ± 4.9 | 1.7 ± 2.7 | 13.5 ± 2.8 |
| Experiment II | L | −31.5 ± 2.2[a] | −60.4 ± 4.2 | −32.8 ± 3.2[a] | −4.7 ± 5.2[a] | 1.1 ± 2.8 | 17.7 ± 2.3[a] |
| | R | 34.0 ± 2.8[a] | 62.4 ± 4.5 | −28.7 ± 3.4[a] | 0.1 ± 5.8[a] | 0.3 ± 4.1 | 16.0 ± 2.8[a] |
| Talairach | R only | 29 | 61 | −35 | −8 | 4–8 | 16 |

In the *x* dimension statistical analysis was performed on absolute min/max values.

[a]Indicates significant differences ($P < 0.05$) between the hemispheres.

with a mean age of 26.3 (range 19–55). All were right-handed as assessed by self-report. Subjects again were drawn from the McGill University and Montreal area population, were paid for their participation and gave informed consent.

### *MR Scanning and Data Manipulation*

Scans were performed on a Philips Gyroscan system with a 1.5 T superconducting magnet using a three-dimensional FFE acquisition sequence to collect 160 contiguous 1 mm, T1-weighted images in the sagittal plane (TR = 18 ms, TE = 10 ms). These data were transformed into standardized stereotaxic space (Talairach and Tournoux, 1988) using an automatic registration program developed at the MNI (Collins *et al.*, 1994). This registration procedure uses a multiscale three-dimensional cross-correlation procedure to match each individual MR volume to the average ($n$ = 305) MR brain volume previously aligned with stereotaxic space. This resampling results in a volume of 160 1 mm slices with an in-plane matrix of 256 × 256.

### *Automatic Grey/White Segmentation*

The anatomical boundaries, methods for marking the scans and DISPLAY software were the same as those used in experiment I. Scans in this sample were marked by a single rater (V.P.). For each scan, the histogram of MR intensities across the full brain volume was generated. Upper and lower intensity boundaries were set from the histogram for voxels to be included in the volume in order to exclude cerebrospinal fluid and artefact. After PAC-r was marked and the total volume measured, the grey/white boundary for the scan was calculated from the histogram by identifying the peak intensity values corresponding to grey and white matter, and taking the mid-point. PAC-r volumes were then automatically segmented, so that voxels with intensity values below the boundary were labelled as grey matter and those with intensity values above the boundary were labelled as white matter. There are many techniques available for tissue segmentation from MR scans, many of which involve multiple acquisitions, which were not available here (for review, see Clarke *et al.*, 1995). Boundaries between the intensity values of different tissue types can also be drawn by picking a minimum value between the two peaks. However, in our data, peak values were more clearly defined than minimum values. In any case, MR intensities are imperfectly correlated with tissue type, and all segmentation techniques result in relative, not absolute values. This technique does not take into account

**Table 2**
Left and right PAC-r volumes and asymmetry coefficients for Experiment I

| Sub | Volume ($mm^3$) | | ∂PAC-r |
|---|---|---|---|
| | Left | Right | |
| 1 | 2528 | 1384 | –0.58 L |
| 2 | 3865 | 1540 | –0.86 L |
| 3 | 1199 | 928 | –0.25 L |
| 4 | 1505 | 1007 | –0.40 L |
| 5 | 2037 | 1734 | –0.16 L |
| 6 | 2545 | 942 | –0.92 L |
| 7 | 3509 | 2157 | –0.48 L |
| 8 | 1460 | 943 | –0.43 L |
| 9 | 3090 | 1166 | –0.90 L |
| 10 | 2768 | 1982 | –0.33 L |
| 11 | 1702 | 1154 | –0.38 L |
| 12 | 1746 | 831 | –0.71 L |
| 13 | 1500 | 748 | –0.67 L |
| 14 | 2248 | 1802 | –0.22 L |
| 15 | 1239 | 1616 | +0.26 R |
| 16 | 1887 | 1823 | –0.03 E |
| 17 | 1239 | 838 | –0.39 L |
| 18 | 2770 | 870 | –1.04 L |
| 19 | 3386 | 1559 | –0.74 L |
| 20 | 1220 | 1550 | +0.24 R |
| Avg | 2172 | 1329 | –0.45 |
| SD | 842 | 437 | 0.36 |

the effect of partial voluming, where voxels containing both grey and white matter have an intermediate intensity, and may be incorrectly classified. However, partial voluming should affect values for grey- and white-matter equally, and should be consistent across the two hemispheres. Importantly, the grey/white border generated by this segmentation showed excellent correspondence with the border as visually identified from the scan (Fig. 5). Separate volumes were then calculated for the grey- and white-matter regions. One subject was excluded from the analysis because the grey/white boundary could not be adequately identified from the histogram. All volume estimates were derived from the MR voxel dimensions ($x$ = 0.67 mm, $y$ = 0.86 mm, $z$ = 0.75 mm). The asymmetry coefficient, ∂PAC-r was calculated for the grey matter, white matter and total volumes (Table 4). The three-dimensional probability map of PAC-r was generated by the same averaging technique used in experiment I (Fig. 2).

## *Results*

### *Probabilistic Mapping*

As described above, Figure 3 presents the contour maps of PAC-r for the regions of 25–50, 50–75 and 75–100% probability in standardized space. The location of PAC-r was again examined using the bounding box for the labelled volumes. Overall, these results were highly consistent with those obtained in experiment I, with the right PAC-r shifted anterior-medially in comparison with the position given in the Talairach atlas, and with left PAC-r (Table 1).

### *Interhemispheric Asymmetries*

Consistent with the previous experiment, the results of experiment II show that the total volume of PAC-r is larger in the left hemisphere, both on average and in the majority of subjects. Analysis of the total volume data using ANOVA for repeated measures showed a significant effect of side [$F(1,18) = 9.9$; $P < 0.006$], with no significant effect of sex [$F(1,18) = 2.7$; $P < 0.11$], or interaction. The majority of individual subjects again had a left-sided asymmetry (12/20 subjects); although a slightly larger number had a right-sided or no asymmetry (R > L in 4/20 subjects; R = L in 4/20 subjects; see Table 4).

Most importantly, separate analysis of grey- and white-matter volumes revealed an interaction between side and tissue type [$F(1,17) = 5.07$, $P < 0.04$] in which the overall asymmetry is the result of larger volumes of cortical white matter in the left PAC-r ($t = -3.95$, $P < 0.001$). The volumes of cortical grey matter were not different for the two hemispheres ($t = -1.39$, $P < 0.18$). The individual values for PAC-r and the asymmetry coefficients for the total, grey- and white-matter volumes are presented in Table 4. The majority of individual subjects showed a left-sided asymmetry in white-matter volume (L > R in 14/20; R > L in 1/20 and R = L in 4/20). Asymmetry measures for grey-matter volumes showed no clear pattern (L > R in 4/20; R > L in 8/20 and R = L in 5/20). Correlations between left and right were significant for the total and grey-matter volumes ($r_{total} = 0.5$; $P < 0.03$; $r_{grey} = 0.5$; $P < 0.03$), and approached significance for the white-matter volumes ($r_{white} = 0.44$; $P < 0.06$). In this sample 60% of the subjects had only one gyrus in both hemispheres (12/20) and 25% had two on the left and one on the right (Table 2). This distribution is consistent with that obtained in experiment I.

## *Discussion*

### *Probabilistic Mapping*

The results of these experiments show that probabilistic mapping in stereotaxic space is an effective method for exploring variation in the location and extent of well-defined anatomical regions in the human brain. Examination of the map and the average location data reveals that PAC-r is located more anterio-medially in the right hemisphere, information that is not available from the commonly used Talairach atlas. This difference (5–8 mm) is large enough that right PAC-r could be incorrectly identified when its location is extrapolated from that of the left. More generally, the probabilistic mapping technique has several advantages over single-brain atlases. First, the variability in location of a particular region can be better estimated because the map includes a sample of individual brains. Second, mapping the probability across a group that a structure will occur at a given voxel location allows statistical evaluation of the location of a region of interest in any brain image that has been transformed into stereotaxic space. We are currently developing statistical methods to quantify the extent of surgical removals in PAC-r from MR scans. Such maps could also be extremely valuable in analysing PET or functional MRI data, where they could be used to assess the location of an activation focus, or to define a region of interest in a directed search or correlational analysis. Finally, manually identified maps such as this one, can serve as models for computer algorithms designed to identify automatically cortical regions from MR scans (Evans *et al.*, 1994; Collins *et al.*, 1995).

### *Interhemispheric Asymmetries*

The results of these experiments show a consistent L > R asymmetry in the total volume of PAC-r, and indicate that this asymmetry results from a larger volume of cortical white matter on the left. As discussed above, varying degrees of asymmetry have been observed in this region since the early part of the century, but the pattern of results has been inconsistent. This inconsistency may be due to variable definitions of the region, and to measurement techniques that were rough or largely descriptive. vonEconomo and Horn (1930) were the first to try to quantify the gross morphology of the region (HG-r) and examine

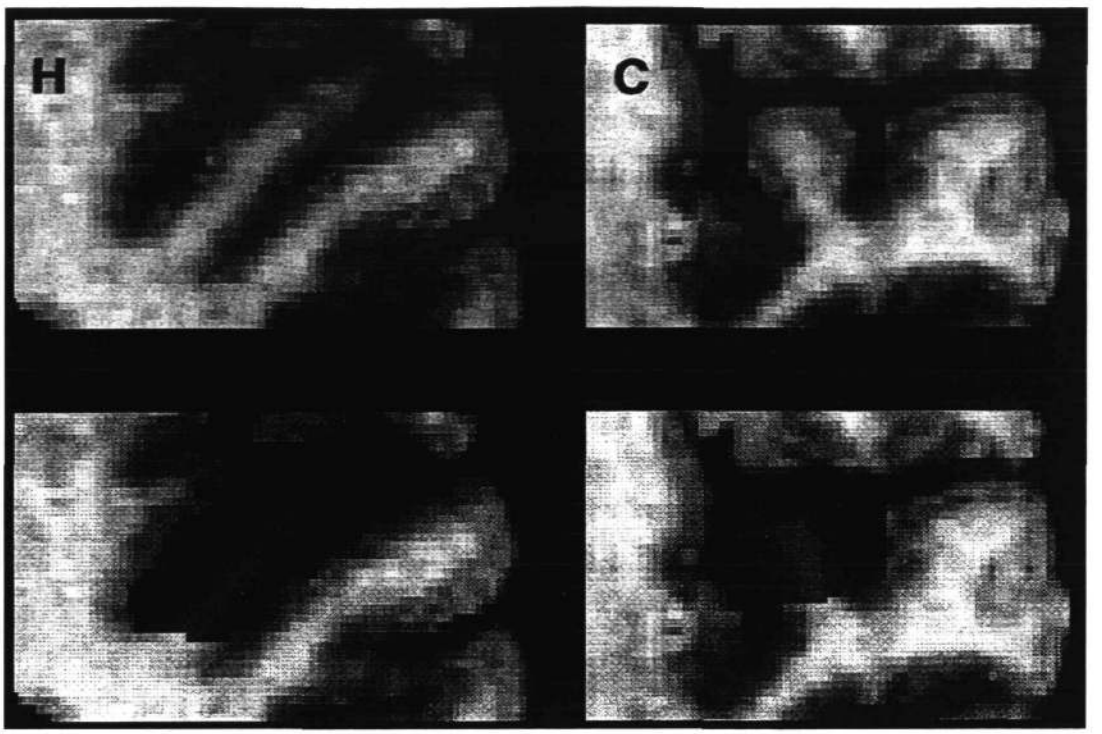


**Figure 5.** Grey/white boundaries for a typical subject in horizontal (H) and coronal (C) sections; medial = left; lateral = right. Upper slices show the grey/white boundaries visually identifiable from 1 mm scans. Lower slices show the results of the automatic segmentation: red = white matter; blue = grey matter.

**Table 3**
Number of HG per hemisphere in the present and previously published investigations

| Author(s) | *n* | No. of HG left/right | | | | |
|---|---|---|---|---|---|---|
| | | 1/2 | 2/2 | 2/1 | 1/1 | Other |
| VonEconomo and Horn (1930) | 11 | 6 (0.55) | 1 (0.09) | 2 (0.18) | 2 (0.18) | 0 |
| Campain and Minkler (1976) | 30 | 14 (0.48) | 11 (0.36) | 1 (0.03) | 3 (0.10) | 1 (0.03) |
| Musiek and Reeves (1990) | 29 | 6 (0.20) | 10 (0.34) | 7 (0.24) | 5 (0.17) | 1 (0.03) |
| Rademacher *et al.* (1993) | 10 | 2 (0.20) | 0 | 3 (0.30) | 4 (0.40) | 1 (0.10) |
| Present study | | | | | | |
| Experiment I | 20 | 4 (0.20) | 1 (0.05) | 1 (0.05) | 14 (0.70) | 0 |
| Experiment II | 20 | 2 (0.10) | 1 (0.05) | 5 (0.25) | 12 (0.60) | 0 |
| *Totals* | *120* | *34 (0.28)* | *24 (0.20)* | *19 (0.16)* | *40 (0.33)* | *3 (0.03)* |

its relationship to PAC. They that found HG-r was often longer and wider on the left, but stated that PAC appeared equal in both hemispheres because it most often covered two gyri on the right and only one on the left. Musiek and Reeves (1990) also found the mean length of HG-r to be greater in the left hemisphere, but did not examine cytoarchitecture. Using gross anatomy alone, Campain and Minkler (1976) found multiple gyri more common on the right, and therefore showed a R > L asymmetry in the surface area of HG-r.

Even those studies which have confined their measurements to either the most anterior HG, or to the cytoarchitectonic region, have produced differing results. Kulynych *et al.* (1994), found no interhemispheric differences when using MR planimetry to examine the surface area of the most anterior HG. The accuracy of surface-rendering is necessarily limited when the region under examination includes cortex which extends below the rendered surface. The typical morphology of PAC-r means that it contains a large proportion of such buried cortex (cf. Fig. 1: coronal section), so that surface-rendering techniques would tend to underestimate it. Further, if the asymmetry in this region is the result of differences in the volume of cortical white matter, measurement of the cortical surface could not detect it. The first estimate of the area of the cytoarchitectonic region of PAC can be made from the data of Galaburda and Sanides (1980), who report measurements for each of the cytoarchitectonic fields they define within auditory cortex. From these data, the total area of PAC (combined areas KAm and KAlt) appears to be equal in the two hemispheres, but only three brains were examined. In the most systematic microscopic investigation to date, Rademacher *et al.* (1993) examined the relative area of PAC and found it to be >10% larger in the left hemisphere of 6/10 cases, although these were relative measurements that could not

**Table 4**
Left and right PAC-r volumes and asymmetry coefficients for experiment II

| Sub | Total Volume | | | Grey volume | | | White volume | | |
|---|---|---|---|---|---|---|---|---|---|
| | L | R | ∂PAC-r | L | R | ∂ | L | R | ∂ |
| 1 | 2159 | 2294 | 0.06 E | 1338 | 1382 | 0.03 E | 821 | 913 | 0.11 R |
| 2 | 1669 | 1961 | 0.16 R | 1289 | 1638 | 0.24 R | 379 | 323 | −0.16 L |
| 3 | 1554 | 1428 | −0.08 E | 1186 | 1245 | 0.05 E | 368 | 183 | −0.67 L |
| 4 | 3563 | 2140 | −0.50 L | 2379 | 1749 | −0.31 L | 1184 | 392 | −1.01 L |
| 5 | 1841 | 1523 | −0.19 L | 1164 | 1224 | 0.05 E | 677 | 298 | −0.78 L |
| 6 | 3895 | 2936 | −0.28 L | 3072 | 2370 | −0.26 L | 822 | 562 | −0.38 L |
| 7 | 1612 | 2151 | 0.29 R | 1234 | 1761 | 0.35 R | 378 | 389 | 0.03 E |
| 8 | 2246 | 2292 | 0.02 E | 1635 | 1676 | 0.02 E | 611 | 616 | 0.01 E |
| 9 | 3210 | 1976 | −0.48 L | 2217 | 1605 | −0.32 L | 993 | 371 | −0.91 L |
| 11 | 1329 | 1647 | 0.21 R | 809 | 1365 | 0.51 R | 522 | 281 | −0.60 L |
| 12 | 5091 | 2869 | −0.56 L | 2654 | 2097 | −0.23 L | 2437 | 778 | −1.03 L |
| 13 | 4139 | 1761 | −0.81 L | 2537 | 1400 | −0.58 L | 1602 | 360 | −1.27 L |
| 14 | 1251 | 1723 | 0.32 R | 884 | 1337 | 0.41 R | 367 | 386 | 0.05 E |
| 16 | 1894 | 2207 | 0.15 R | 1116 | 1683 | 0.41 R | 778 | 524 | −0.39 L |
| 17 | 3587 | 1390 | −0.88 L | 2480 | 1073 | −0.79 L | 1108 | 317 | −1.11 L |
| 18 | 3108 | 1975 | −0.45 L | — | — | — | — | — | — |
| 19 | 2578 | 1751 | −0.38 L | 1463 | 1423 | −0.03 E | 1115 | 328 | −1.09 L |
| 20 | 1997 | 1364 | −0.38 L | 1565 | 1183 | −0.28 L | 432 | 181 | −0.82 L |
| 21 | 2224 | 1745 | −0.24 L | 1545 | 1452 | −0.06 E | 679 | 293 | −0.79 L |
| 22 | 2125 | 1354 | −0.44 L | 1574 | 982 | −0.46 L | 551 | 372 | −0.39 L |
| Avg | 2554 | 1924 | −0.22 | 1692 | 1508 | −0.07 | 833 | 414 | −0.59 |
| SD | 1057 | 454 | 0.36 | 659 | 342 | 0.38 | 514 | 189 | 0.43 |

be analysed statistically. While their L > R asymmetry in PAC is broadly consistent with our own results, we did not find a specific grey-matter asymmetry. This discrepancy could be attributable to our definition of the region from gross anatomical landmarks. In those cases where PAC spreads beyond the landmarks, our technique would underestimate its extent. Alternately, because our definition of PAC-r comprises all of the most anterior HG, it almost certainly includes non-koniocortical auditory fields usually located on the lateral surface of this gyrus [area 42 of Brodmann (1909); or PaAlt of Galaburda and Sanides (1980)]. Inclusion of this lateral region may obscure differences in grey-matter volume that would be observable if PAC were examined alone. Therefore, it is possible that in addition to the observed white-matter asymmetry in PAC-r overall, there is also a specific grey-matter asymmetry for PAC alone.

Our findings reveal an anatomical asymmetry that arises from a difference in the volume of cortical fibres that carry information to and from PAC-r. We cannot determine whether this asymmetry reflects thalamocortical or corticocortical connections. Greater myelination of thalamocortical input to left PAC-r could allow faster conduction of nerve impulses, which might be detectable as shorter latencies in early components of auditory evoked potentials (AEPs). No specific investigation of this question has been made to date, but results of depth-electrode recordings in HG-r show no differences in AEP latencies between the two hemispheres (Liégeois-Chauvel *et al.*, 1994), although no statistical comparison was made. On the other hand, it is tempting to consider that this asymmetry may be related to intrinsic connections to the adjacent PT (area 22), which is consistently larger in the left hemisphere. PAC is known to be densely interconnected with all adjacent auditory regions (cf. Cipolloni and Pandya, 1989), and it therefore seems likely that a larger number of fibres connect the left PAC to the larger left PT.

Quantitative cytoarchitectonic studies in the human brain show evidence of differential cellular organization in the left and

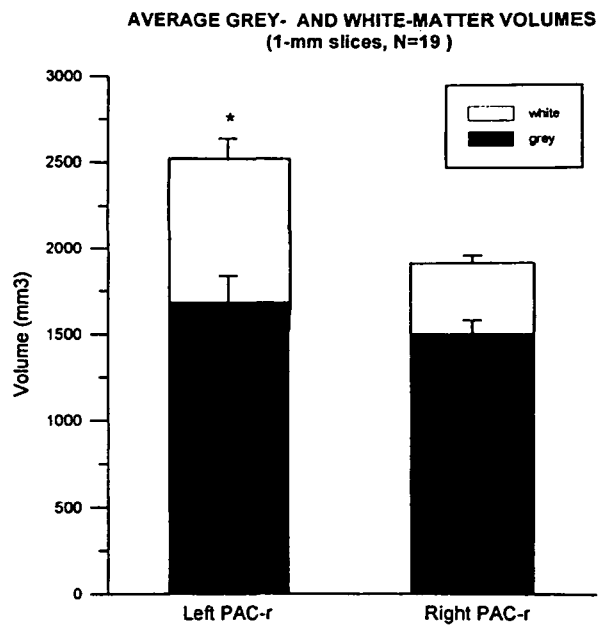


**Figure 6.** Average volumes of grey and white matter for left and right PAC-r in Experiment II. Standard errors displayed as vertical bars.

right auditory cortices. Seldon (1981a,b, 1982) showed that the cell columns of the left PAC are both wider, and more widely spaced, than those of the right. Further, he found that an individual column on the left was contacted by more afferents than a similar cell column on the right. Thus, given a similar number of cell bodies (grey matter), the amount of neuropil (white matter) is greater on the left, and this neuropil is more densely packed with neuronal processes. In related work, Galuske *et al.* (1995) have shown a L > R asymmetry in the

spacing of patches of intrinsic connections to adjacent area 22 (PT). The wider spacing of these patches could be the result of larger left PAC projection columns. Finally, Hutsler and Gazzaniga (1996) have shown a L > R asymmetry in the size of layer III pyramidal cells in PAC, and other areas of auditory cortex. Such large cells would be likely to form larger columns, and to send out thicker or more heavily branched axons to other regions of auditory cortex.

The functional significance of such asymmetries in the size and organization the auditory cortices is not clearly known. Although the L > R asymmetry of the PT has long been linked to the left-hemisphere specialization for speech (Geschwind and Levitsky, 1968; Witelson and Pallie, 1973; Steinmetz *et al.*, 1989b), direct evidence for the relation of this structural difference to functional difference is still fragmentary (Ratcliff *et al.*, 1980; Foundas *et al.*, 1994). In order to understand left-hemisphere specialization for speech more precisely, researchers have focused on identifying acoustic parameters that are required to discriminate speech sounds. One important characteristic of speech sounds is that they often differ only over short, rapidly changing segments–usually consonants. In order to distinguish one speech sound from another, the auditory cortex must be able to encode these rapid temporal changes precisely. Multi-unit recordings from PAC of the macaque monkey show time-locked responses to temporal components of auditory stimuli that are related to consonant discrimination (Steinschneider *et al.*, 1995). A number of investigators have hypothesized that an enhanced capacity to analyse and encode temporal aspects of acoustic information may underlie the left temporal lobe's contribution to speech functions. Studies with aphasic (Efron, 1963), and left-hemisphere-damaged subjects (Robin *et al.*, 1990) have shown an impairment in the capacity to perceive specifically temporal components of auditory information. Tallal and her colleagues have found evidence for interference in the perception and production of the rapid temporal component of speech sounds in language-impaired children and adults (for review, see Tallal *et al.*, 1993). These data support a preferential role for the left hemisphere in the fine-grained analysis of temporal aspects of auditory stimuli. It is possible that the observed structural differences in the organization of the left auditory cortices underlie this differential capacity.

Thus far, we have interpreted our data as reflecting part of the innate anatomical basis of left-hemisphere specialization for speech. This interpretation is supported by differences found in adult, newborn and fetal tissue (cf. Chi *et al.*, 1973; Witelson and Pallie, 1973; Galaburda *et al.*, 1978). However, the structural differences observed in adults may also be related to the development of speech functions which themselves produce changes in the underlying cortex. Experiments in animals have convincingly shown that changes in cortical mapping can occur over brief periods of time, and are long-lasting (for review, see Merzenich *et al.*, 1990). Recordings in guinea-pig auditory cortex have shown changes in the tuning of single neurons with conditioning (Bakin and Weinberger, 1990), and experiments with monkeys have shown changes in the extent of cortical representation of a tone related to discrimination learning (Recanzone *et al.*, 1993). In this context, it seems likely that it is an interaction between innate structural specialization, and specialization mediated by use which produces the final adult cortical structure.

In conclusion, the observed asymmetry in the volume of white matter in PAC-r may be the result of differences in the cellular organization of the two hemispheres. These structural differences may in turn contribute directly to enhanced left-hemisphere processing of temporal aspects of auditory stimuli. In information-processing terms, the specialized neuronal circuitry of the left auditory cortices would facilitate the transduction and transmission of temporal aspects of auditory information. Therefore, the anatomical differences that are relevant for speech perception may be related not only to the extent of the cytoarchitectonic areas which perform these computations, but to the number and organization of their connections.

## Notes

We would like to thank Ms Avital Fleischer for her assitance in labelling the scans. The research described in this paper was supported by grants from the McDonnell-Pew Program in Cognitive Neuroscience, the Human Brain Map Project, the Medical Research Council of Canada (MT11541 and SP30), and the National Institutes of Health/Mental Health (MH10817-01A1).

Correspondence should be addressed to Virginia Penhune, Department of Neuropsychology, Room 183, Montréal Neurological Institute, 3801 University, Montréal, Québec, Canada H3A 2B4.

## References

Bakin JS, Weinberger NM (1990) Classical conditioning induces CS-specific receptive field plasticity in the auditory cortex of the guinea pig. Brain Res 536:271-286.

Braak H (1978) On magnopyramidal temporal fields in the human brain–probable morphological counterparts of Wernicke's sensory speech region. Anat Embryol 152:141-169.

Brodmann K (1909) Vergleichende Lokalisationslehre der Grosßhirnrinde. Leipzig: Barth.

Campain R, Minkler J (1976) A note on the gross configurations of the human auditory cortex. Brain Lang 3:318-323.

Celesia G (1976) Organization of auditory cortical areas in man. Brain 99:403-414.

Chi JG, Dooling EC, Gilles FH (1973) Left-right asymmetries of the temporal speech areas of the human fetus. Arch Neurol 34:346-348.

Cipolloni PB, Pandya DN (1989) Connectional analysis of the ipsilateral and contralateral afferent neurons of the superior temporal region in the rhesus monkey. J Comp Neurol 281:567-585.

Clarke LP, Velthuizen RP, Camacho MA, Heine JJ, Vaidyanathan M, Hall LO, Thatcher RW and Silbiger RW (1995) MRI segmentation: Methods and applications. Magn Reson Imag 13:343-368.

Collins DL, Neelin P, Peters TM, Evans AC (1994) Automatic 3D intersubject registration of MR volumetric data in standardized Talairach space. J Comput Assist Tomogr 18:192-205.

Collins DL, Holmes C, Peters TM, Evans AC (1995) Automatic 3D model-based neuroanatomical segmentation. Hum Brain Mapping 3:190–208.

vonEconomo C and Koskinas GH (1925) Die Cytoarchitektonik der Hirnrinde des Erwachsenen Menschen. Wien: Springer.

vonEconomo C, Horn L (1930) Über Windungsrelief, Maße und Rindenarchitektonik der Supratemporalfläche, ihre individuellen und ihre Seitenunterschiede. Z Neurol Psychiat 130:678-757.

Efron R (1963) Temporal perception, aphasia and déjà vu. Brain 86:403-423.

Evans AC, Marrett S, Neelin P, Collins L, Worsley K, Dai W, Milot S, Meyer E, Bub D (1992a) Anatomical mapping of functional activation in stereotactic coordinate space. NeuroImage 1:43-53.

Evans AC, Collins DL, Milner B (1992b) An MRI-based brain atlas from 300 young normal subjects. Soc Neurosci Abstr 18:408.

Evans AC, Kamber M, Collins DL, MacDonald D (1994) An MRI-based probabilistic atlas of neuroanatomy. In: Magnetic resonance scanning and epilepsy (Shorvan et al, eds). New York: Plenum Press, pp 263-274.

Flechsig P (1908) Bemerkungen über die Hörsphäre des menschlichen Gehirns. Neurol Zentralbl 27: 2-7.

Foundas AL, Leonard CM, Gilmore R, Fennell E and Heilman KM (1994) Planum temporale asymmetry and language dominance. Neuropsychologia 32:1225-1231.

Galaburda AM, Sanides F, Geschwind N (1978) Cytoarchitectonic

left–right differences in the temporal speech region. Arch Neurol 35:812-817.
Galaburda AM, Sanides F (1980) Cytoarchitectonic organization of the human auditory cortex. J Comp Neurol 190:597-610.
Galuske RAW, Scholote W, Singer W (1995) Interhemispheric differences of patchy intrinsic connections in Wernicke's area (area 22) of the human brain. Soc Neurosci Abstr 22(1):675.
Geschwind N and Levitsky W, (1968) Human brain: left-right asymmetries in the temporal speech region. Science 161:186-187.
Hopf A (1968) Photometric studies on the myeloarchitecture of the human temporal lobe. J Hirnforsch 10:285-297.
Hutsler JJ, Gazzaniga MS (1996) Acetylcholinesterase staining in human auditory and language cortices–regional variation of structural features. Cereb Cortex 6:260-270.
Kulynych JJ, Vladar K, Jones DW, Weinberger (1993) Three-dimensional surface rendering in MRI morphometry: a study of the planum temporale. J Comput Assist Tomgr 17:529-535.
Kulynych JJ, Vladar K, Jones DW, Weinberger DR (1994) Gender differences in the normal lateralization of the supratemporal cortex: MRI surface-rendering morphometry of Heschl's gyrus and the planum temporale. Cereb Cortex 4:107-118.
Lauter JL, Herscovitch P, Formby C, Raichle, ME (1985) Tonotopic organization in human auditory cortex revealed by PET. Hearing Res 20:199-205.
Liégeois-Chauvel C, Musolino A, Chauvel P (1991) Localization of the primary auditory area in man. Brain 114:139-153.
Liégeois-Chauvel C, Musolino A, Badier JM, Marquis P, Chauvel P (1994) Evoked potentials recorded from the auditory cortex in man: evaluation and topography of the middle latency components. Electroencephalogr Clin Neurophysiol 92:204-214.
Luria AR (1973) The working brain. New York: Basic Books.
MacDonald JD, Avis D, Evans AC (1994) Multiple surface identification and matching in magnetic resonance images. Proc Soc Vis Biomed Comput 160-169.
Merzenich MM, Recanzone GH, Jenkins WM, Grajski KA (1990) Adaptive mechanisms in the cortical networks underlying cortical contributions to learning and nondeclarative memory. Cold Spring Harb Symp Quant Biol 15:873-887.
Musiek FE, Reeves AG (1990) Asymmetries of the auditory areas of the cerebrum. J Am Acad Audiol 1:240-245.
Paus T, Tomaiuolo F, Otaky N, MacDonald JD, Petrides M, Atlas J, Morris R, Evans AC (1996) Human cingulate and paracingulate sulci: pattern, variability, asymmetry and probabilistic map. Cereb Cortex 6:207-214.
Pfeifer RA (1920) Myelogenetisch-anatomische Untersuchungen über das kortikale Ende der Hörleitung. Abh Math-Physik Kl sächs Akad Wiss Leipzig 37:1-54.
Pfeifer RA (1936) Pathologie der Hörstrahlung und der corticalen Hörsphäre. In: Handbuch der Neurologie, Vol 6 (Bumke O, Foerster O, eds), pp 533-636. Berlin: Springer-Verlag.
Rademacher J, Caviness VS, Steinmetz H, Galaburda AM (1993) Topographical variation of the human primary cortices: omplications for neuroimaging, brain mapping and neurobiology. Cereb Cortex 3:313-329.
Ratcliff G, Dila C, Taylor L and Milner BM (1980) The morphological asymmetry of the hemispheres and cerebral dominance for speech: a possible relationship. Brain Lang 11:87-98.
Recanzone GH, Schreiner CE, Merzenich MM (1993) Plasticity in the frequency representation of primary auditory cortex following discrimination training in adult owl monkeys. J Neurosci 13:87-103.
Robin DA, Tranel D, Damasio H (1990) Auditory perception of temporal and spectral events in patients with focal left and right cerebral lesions. Brain Lang 39:539-555.
Sanides F (1975) Comparative Neurology of the temporal lobe in primates including man with reference to speech. Brain Lang 2:396-419.
Seldon HL (1981a) Structure of human auditory cortex I: Cyto-architectonics and dendritic distributions. Brain Res 229:277-294.
Seldon HL (1981b) Structure of human auditory cortex II: axon distributions and morphological correlates of speech perception. Brain Res 229:295-310.
Seldon HL (1982) Structure of human auditory cortex III: statistical analysis of dendritic trees. Brain Res 249:211-221.
Steinmetz H, Furst G, Freund H-J (1989a) Application and validation of the proportional grid system in MR imaging. J Comput Assist Tomgr 13:10-19.
Steinmetz H, Rademacher J, Huang Y, Hefter H, Zilles K, Thron A, Freund H-J (1989b) Cerebral asymmetry: MR planimetry of the human planum temporale. J Comput Assist Tomgr, 13:996-1005.
Steinmetz H, Rademacher J, Janke L, Huang Y, Thron A, Zilles K (1990) Total surface of temporoparietal intrasylvian cortex: Diverging left–right asymmetries. Brain Lang 39:357-372.
Steinschneider M, Schroeder CE, Arezzo JC, Vaughan HG (1995) Physiologic correlates of the voice onset time boundary in primary auditory cortex of the awake monkey: temporal response patterns. Brain Lang 48:326-340.
Talairach J, Szikla G, Tournoux P, Prossalentis A, Bordas-Ferrer M, Covello L, Jacob M, Mempel A (1967) Atlas d'anatomie stéréotaxique du télencéphale. Paris: Masson.
Talairach J, Tournoux P (1988) Co-planar stereotaxic atlas of the human brain. New York: Thieme.
Tallal P, Miller S, Fitch RH (1993) Neurobiological basis of speech: A case for the preeminence of temporal processing. Ann NY Acad Sci 682:27-47.
Wernicke, C (1874) In: Der aphasische Symptomencomplex (Cohn M, Weigert, eds). Breslau, Poland.
Witelson SF, Pallie W, 1973. Left hemisphere specialization for language in the newborn. Neuroanatomical evidence of asymmetry. Brain 96:641-646.
Zatorre RJ, Evans AC, Meyer E, Gjedde A (1992) Lateralization of phonetic and pitch discrimination in speech processing. Science 256:846-849.